thus minimizing the dose to surrounding normal tissues. We note that *p*-SCN-Bz-DTPA is the most stable chelate available for ^{212}Bi. Finally, current studies[71] with the β-emitter ^{90}Y indicate a pattern of stability for the various chelates similar to that reported here for ^{111}In. A detailed investigation of in vivo stability of protein-linked therapeutic radionuclides is under way.

Acknowledgment. The authors acknowledge the assistance of Dr. Henry Fales, Laboratory of Chemistry, National Heart, Lung, and Blood Institute, NIH, for assistance in obtaining mass spectra. We thank Dr. Andrew Keenan, Nuclear Medicine Department, Clincical Center, NIH, for help with γ-camera imaging.

Registry No. **1**, 102650-30-6; **2**, 94344-71-5; **4**, 17193-40-7; **5**, 81677-61-4; **6**, 96813-21-7; **7**, 81677-63-6; **8**, 81677-65-8; **9**, 96813-44-4; **10**, 102650-28-2; **11**, 96813-40-0; **12**, 102650-29-3; **13**, 33305-77-0; *p*-$BrCH_2CONHC_6H_4CH_2CH(N(CH_2CO_2H)_2)CH_2N(CH_2CO_2H)_2$, 81677-64-7.

Supplementary Material Available: Tables of analytical and mass spectral data and a figure showing NMR spectra (3 pages). Ordering information is given on any current masthead page.

(71) Strand, M.; et al., private communication.

Contribution from the Department of Chemistry, Michigan State University, East Lansing, Michigan 48824, Department of Chemistry, University of Virginia, Charlottesville, Virginia 22901, and AT&T Bell Laboratories, Murray Hill, New Jersey 07974

X-ray Absorption Studies of the Purple Acid Phosphatase from Beef Spleen

S. M. Kauzlarich,[1a,b,2a] B. K. Teo,*[3] T. Zirino,[2a] S. Burman,[2a,b] J. C. Davis,[1a,c] and B. A. Averill*[2a,4]

Received April 4, 1986

Iron K-edge near-edge (XANES) and extended X-ray absorption fine structure (EXAFS) spectra have been measured for the purple acid phosphatase from beef spleen and for several oxo-bridged model complexes. The XANES show a shift of the absorption edge to lower energy by 2.0 eV upon reduction of the purple form of the enzyme to the pink form, consistent with reduction of one of the iron atoms. Fourier transforms of the EXAFS data of the purple form of the enzyme show three peaks, assigned to Fe–O(N) (first shell), Fe--Fe and Fe--P or Fe--C (second shell), and Fe--C(N) (imidazole, third shell) scatterers, in order of increasing distance. Best fits of the individually back-transformed peaks using theoretical functions are consistent with the indicated assignments. The Fe--Fe distance of 3.00 Å is consistent with a bridged binuclear iron center in the enzyme. Due to the presence of short Fe–O(tyrosine) linkages at 1.8–1.9 Å, direct evidence for a bridging oxo group at ca. 1.8 Å could not be obtained. The observed Fe--P distance of 3.06 Å is most consistent with the presence of a phosphate as a monodentate ligand to one iron atom in the purple (oxidized) form of the enzyme.

Purple acid phosphatases are characterized by their intense ($\epsilon \sim 4000\ M^{-1}\ cm^{-1}$) absorption band at 510–550 nm.[5] Their presence in mammalian, plant, and microbial sources[5,6a] suggests that these enzymes are of primary importance in the regulation of the physiological level of inorganic phosphate and phosphorylated metabolites. The enzymes from beef spleen[6] and porcine uterine fluid[6d,7] both contain diiron centers, whereas the enzyme from sweet potato is reported to contain manganese.[8] Electron paramagnetic resonance spectra[6e,9] and magnetic susceptibility studies[9] of the enzyme isolated from beef spleen are consistent with the oxidized (purple) enzyme containing an antiferromagnetically coupled $[Fe^{III}]_2$ unit and the enzymatically active, reduced (pink) enzyme containing a spin-coupled mixed-valence Fe(III)–Fe(II) unit. A similar picture is now accepted for the porcine uterine enzyme.[10] The EPR spectra and magnetic properties of the semimet form of hemerythrin[11] are very similar to those observed in the purple acid phosphatase from beef spleen and porcine uterine fluid, suggesting the existence of a related binuclear unit in all three proteins. Results from resonance Raman studies have established the presence of tyrosine ligands to iron in both the porcine[12] and beef spleen[13] enzymes. On the basis of proton NMR spectra, both histidine and tyrosine groups are suggested to be bound to the iron of the porcine enzyme.[14] EPR and UV–visible absorption studies of phosphate binding indicate that phosphate binds near, if not at, the iron site.[7,9,15] Magnetic

(1) (a) Michigan State University. (b) Current address: Department of Chemistry, Iowa State University, Ames, IA 50010. (c) Current address: SOHIO Research Center, Cleveland, OH 44128.
(2) (a) University of Virginia. (b) Current address: Department of Biochemistry, Cornell Medical Center, New York, NY 10021.
(3) AT&T Bell Laboratories. Current address: Department of Chemistry, University of Illinois at Chicago, Box 4348, Chicago, IL 60680.
(4) A. P. Sloan Foundation Fellow, 1981–1985.
(5) Antanaitis, B. C.; Aisen, P. *Adv. Inorg. Biochem.* **1983**, *5*, 111–136.
(6) (a) Davis, J. C.; Lin, S. S.; Averill, B. A. *Biochemistry* **1981**, *20* 4062–4067. (b) Glomset, J.; Porath, J. *Biochim. Biophys. Acta* **1960**, *39*, 1–8. (c) Campbell, H. D.; Zerner, B. *Biochem. Biophys. Res. Commun.* **1973**, *54*, 1498–1503. (d) Campbell, H. D.; Dionysius, D. A.; Keough, D. T.; Wilson, B. E.; de Jersey, J.; Zerner, B. *Biochem. Biophys. Res. Commun.* **1978**, *82*, 615–620. (e) Antanaitis, B. C.; Aisen, P. *J. Biol. Chem.* **1982**, *257*, 5330–5332.
(7) (a) Schlosnagle, D. C.; Bazer, F. W.; Tsibris, J. C. M.; Roberts, R. M. *J. Biol. Chem.* **1974**, *249*, 7574–7579. (b) Schlosnagle, D. C.; Sander, E. G.; Bazer, F. W.; Roberts, R. M. *J. Biol. Chem.* **1976**, *251*, 4680–4685. (c) Keough, D. T.; Dionysius, D. A.; de Jersey, J.; Zerner, B. *Biochem. Biophys. Res. Commun.* **1980**, *94*, 600–605. (d) Antanaitis, B. C.; Aisen, P.; Lilienthal, H. R.; Roberts, R. M.; Bazer, F. W. *J. Biol. Chem.* **1980**, *255*, 11204–11209. (e) Antanaitis, B. C.; Aisen, P. *J. Biol. Chem.* **1982**, *257*, 1855–1859.
(8) (a) Uehara, K.; Fujimoto, S.; Taniguchi, T. *J. Biochem. (Tokyo)* **1974**, *75*, 627–638. (b) Sugiura, Y.; Kawabe, H.; Tanaka, H. *J. Am. Chem. Soc.* **1980**, *102*, 6581–6582. (c) Sugiura, Y.; Kawabe, H.; Tanaka, H.; Fujimoto, S.; Ohara, A. *J. Am. Chem. Soc.* **1981**, *103*, 963–964. (d) Sugiura, Y.; Kawabe, H.; Tanaka, H.; Fujimoto, S.; Ohara, A. *J. Biol. Chem.* **1981**, *256*, 10664–10670. (e) Kawabe, H.; Sugiura, Y.; Terauchi, M.; Tanaka, H. *Biochim. Biophys. Acta* **1984**, *784*, 81–89.
(9) Davis, J. C.; Averill, B. A. *Proc. Natl. Acad. Sci. U.S.A.* **1982**, *79*, 4623–4627.
(10) (a) Antanaitis, B. C.; Aisen, P.; Lilienthal, H. R. *J. Biol. Chem.* **1983**, *258*, 3166–3172. (b) Antanaitis, B. C.; Aisen, P. *J. Biol. Chem.* **1984**, *259*, 2066–2069. (c) Sinn, E.; O'Connor, C. J.; de Jersey, J.; Zerner, B. *Inorg. Chim. Acta* **1983**, *78*, L13–L15. (d) Debrunner, P. G.; Hendrich, M. P.; de Jersey, J.; Keough, D. T.; Sage, J. T.; Zerner, B. *Biochim. Biophys. Acta* **1983**, *745*, 103–106.
(11) Muhoberac, B. B.; Wharton, D. C.; Babcock, L. M.; Harrington, P. C.; Wilkins, R. G. *Biochim. Biophys. Acta* **1980**, *626*, 337–345.
(12) (a) Gaber, B. P.; Sheridan, J. P.; Bazer, F. W.; Roberts, R. M. *J. Biol. Chem.* **1979**, *254*, 8340–8342. (b) Antanaitis, B. C.; Strekas, T.; Aisen, P. *J. Biol. Chem.* **1982**, *257*, 3766–3770.
(13) Averill, B. A.; Davis, J. C.; Burman, S.; Zirino, T.; Sanders-Loehr, J.; Loehr, T. M.; Sage, J. T.; Debrunner, P. G., submitted for publication.
(14) Lauffer, R. B.; Antanaitis, B. C.; Aisen, P.; Que, L., Jr. *J. Biol. Chem.* **1983**, *258*, 14212–14218. Similar spectra have been observed for the beef spleen enzyme (Que, L. Jr.; Averill, B. A., unpublished results).
(15) (a) Keough, D. T.; Beck, J. L.; de Jersey, J.; Zerner, B. *Biochem. Biophys. Res. Commun.* **1982**, *108*, 1643–1648. (b) Antanaitis, B. C.; Aisen, P. *J. Biol. Chem.* **1983**, *260*, 751–756. (c) Burman, S.; Davis, J. C.; Weber, M. J.; Averill, B. A. *Biochem. Biophys. Res. Commun.* **1986**, *136*, 490–497.

0020-1669/86/1325-2781$01.50/0

susceptibility data gave a value of $-2J \geq 100$ cm^{-1} for the purple form of the bovine enzyme,[9] indicative of a substantial antiferromagnetic exchange interaction. Analysis of the extended X-ray absorption fine structure (EXAFS) has aided in the elucidation of the structure of the iron center of hemerythrin.[16] Although an analogous μ-oxo-bridged iron complex has been proposed for the purple phosphatases,[10c,17] direct structural evidence is lacking. We report herein the results of X-ray absorption spectroscopy studies on the purple acid phosphatase from beef spleen, which support the presence of a binuclear iron site in which the iron atoms may be multiply bridged.

Experimental Section

Acid Phosphatase. The purple acid phosphatase from beef spleen (hereafter abbreviated as FePase) was prepared and assayed as described.[6a] The pink form was prepared by reduction of dilute (ca. 25 μM) solutions with excess ascorbate and ferrous ammonium sulfate, followed by concentration (Amicon PM-10), desalting (Sephadex G-25), and further concentration (Amicon PM-10). Samples of both purple and pink forms of the enzyme were ~4 mM in iron.

Model Compounds. $[Fe(2\text{-Mequin})_2]_2O$[18] (2-Mequin = 8-hydroxy-2-methylquinolinate) (I), $[(N\text{-}(n\text{-propyl})sal)_2Fe]_2O$[19] (sal = salicylaldiminate) (II), $[(N\text{-}(p\text{-chlorophenyl})sal)_2Fe]_2O$[20] (III), $enH_2[Fe(HEEDTA)_2]O$[21] (en = ethylenediamine, HEEDTA = *N*-(hydroxyethyl)-ethylenediaminetriacetate (VI), and $[Fe(HB(pz)_3)(O_2CCH_3)]_2O$[22] (pz = pyrazolyl) (V) were prepared according to published procedures.

X-ray Absorption Measurements. X-ray absorption spectra were collected at CHESS (Cornell High-Energy Synchrotron Source) operating at 4.73 GeV with a typically 28–30-mA electron-beam current. The measurements were performed on beam line C-1, which was equipped with an Si(111) monochromator. Fluorescence spectra on protein and model compounds were collected at -80 ± 1 °C, using an ion chamber equipped with Soller slits (based on the design of Stern and Heald[24]). Spectra were obtained on three different occasions on several different sample preparations to ensure reproducibility. The model compounds were diluted with boron nitride and pressed into homogeneous pellets. All samples were contained in plexiglass cells ($19 \times 5 \times 3$ mm^3 sample volume). The spectra of the model compounds were obtained under conditions similar to those of the enzyme. All spectra were measured by using a beam width of 12 mm and a resolution of 1–2 eV. The monochromator was detuned by ca. 30% to minimize contributions from higher harmonics, without significant loss of intensity. Typical spectra were collected from 7020 to 7800 eV during 18–23 min. Eleven spectra of the purple form of FePase, six of the pink form, and two of each of the model compound were averaged for analysis. The integrity of the enzyme samples was checked by measurement of optical spectra and enzymatic activity after thawing; no evidence for bleaching or photoreduction was observed. The data were analyzed at Bell Laboratories, Murray Hill, NJ, by using data reduction[25] and curve-fitting[26] programs described elsewhere[27] and adapted to run on a DEC PDP 11/34 minicomputer.

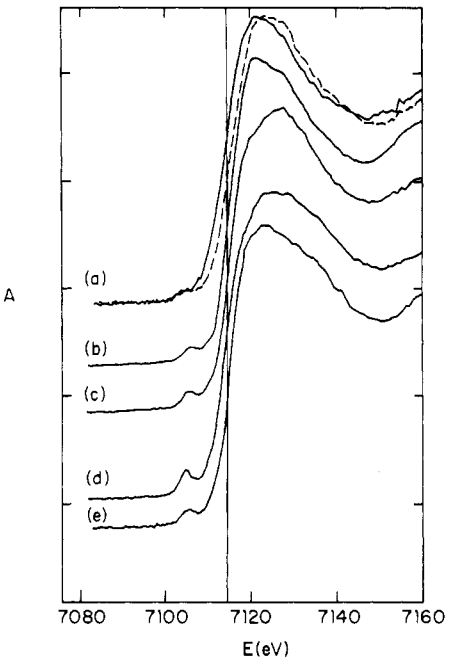

Figure 1. Fe K-edge spectra: (a) pink (solid line) and purple (dashed line) FePase; (b) $[Fe(HB(pz)_3)(O_2CCH_3)]_2O$ (V); (c) $[Fe(N\text{-}(n\text{-propyl})sal)_2]_2O$ (II); (d) $[Fe(2\text{-Mequin})_2]_2O$ (I); (e) enH_2 $[Fe(HEEDTA)]_2O$ (IV). The ordinate is an arbitrary absorbance scale.

Results and Discussion

Near-Edge Structure. The near-edge region of the X-ray absorption spectrum can provide information on the oxidation state and coordination geometry of the absorbing atom.[28] Figure 1 shows the X-ray absorption edge spectra of the purple and pink forms of FePase, as well as those of several model compounds. The absorption edge of the pink form is shifted to lower energy by 2.0 ± 0.5 eV, consistent with reduction of one of the Fe(III) ions to Fe(II).[29]

The most obvious feature is the 1s → 3d peak,[30] located ca. 10 eV below the edge. This transition is forbidden by dipole selection rules, but occurs due to quadrupole and symmetry-breaking effects.[30] The peak is most intense for tetrahedrally coordinated iron atoms such as that found in the Fe–S protein rubredoxin[30] and less intense in the non-heme iron dioxygenases[28] and in the diiron protein hemerythrin,[16b] implying an inversion-asymmetric pseudooctahedral geometry around the iron atoms

(16) (a) Hendrickson, W. A.; Co, M. S.; Smith, J. L.; Hodgson, K. O.; Klippenstein, G. L. *Proc. Natl. Acad. Sci. U.S.A.* **1982**, *79*, 6255–6259. (b) Elam, W. T.; Stern, E. A.; McCallum, J. D.; Sanders-Loehr, J. *J. Am. Chem.* Soc. **1982**, *104*, 6369–6373. (c) Elam, W. T.; Stern, E. A.; McCallum, J. D.; Sanders-Loehr, J. *J. Am. Chem. Soc.* **1983**, *105*, 1919–1923.

(17) Mockler, G. M.; de Jersey, J.; Zerner, B.; O'Connor, C. J.; Sinn, E. *J. Am. Chem. Soc.* **1983**, *105*, 1891–1893.

(18) Mabbs, F. E.; McLachlan, V. N.; McFadden, D.; McPhail, A. T. *J. Chem. Soc., Dalton Trans.* **1973**, 2016–2021.

(19) Davies, J. E.; Gatehouse, B. M. *Cryst. Struct. Commun.* **1972**, *1*, 115–120.

(20) Davies, J. E.; Gatehouse, B. M. *Acta Crystallogr., Sect. B: Struct. Crystallogr. Cryst. Chem.* **1973**, *B29*, 2651–2658.

(21) Lippard, S. J.; Schugar, H.; Walling, C. *Inorg. Chem.* **1967**, *6*, 1825–1831.

(22) (a) Armstrong, W. H.; Lippard, S. J. *J. Am. Chem. Soc.* **1983**, *105*, 4837–4838. (b) Armstrong, W. H.; Spool, A.; Papaefthymiou, G. C.; Frankel, R. B.; Lippard, S. J., *J. Am. Chem. Soc.* **1984**, *106*, 3653–3667.

(23) Stern, E. A.; Elam, W. T.; Bunker, B. A.; Lu, K. O.; Heald, S. M. *Nucl. Instrum. Methods Phys. Res.* **1982**, *195*, 345–356.

(24) Stern, E. A.; Heald, S. M. *Rev. Sci. Instrum.* **1979**, *50*, 1579–1582.

(25) For conversion to k space ($k = [(2m/\hbar^2)(E - E_0^{expt})]^{1/2}$), the experimental energy threshold was chosen at 7111 eV (the energy at half-height of the edge jump). The data were weighted by k^3, and the background was removed by using four sets (3.45 Å^{-1} each) of cubic spline functions. The EXAFS was normalized by dividing by the edge jump.

(26) (a) The nonlinear least-squares refinement of the scale factors (independent of the photoelectron wave vector k_j) for the scattering atoms of the jth type B_j, at distances r_j from the absorbing atom, the root-mean-square relative displacements σ_j (Debye–Waller factors), along r_j and the threshold energy differences, ΔE_{0j}, was based upon the minimization of the sum of the squares of the residuals, $\sum^2 = \sum[k^3\chi(k)_i - k^3\chi'(k)_i]^2$. $k^3\chi(k)_i$ and $k^3\chi'(k)_i$ are the calculated and the observed EXAFS, respectively, and i runs through each data point. (b) Teo, B. K; Antonio, M. R.; Averill, B. A. *J. Am. Chem. Soc.* **1983**, *105*, 3751–3762. (c) Antonio, M. R.; Teo, B. K.; Orme-Johnson, W. H.; Nelson, M. J.; Groh, S. E.; Lindahl, P. A.; Kauzlarich, S. M.; Averill, B. A. *J. Am. Chem. Soc.* **1982**, *104*, 4703–4705.

(27) (a) Teo, B. K.; Antonio, M. R.; Coucouvanis, D.; Simhon, E. D.; Strempler, P. P. *J. Am. Chem. Soc.* **1983**, *105*, 5767–5770. (b) Teo, B. K.; Chen, H. S.; Wang, R.; Antonio, M. R. *J. Non-Cryst. Solids* **1983**, *58*, 249–274. (c) Antonio, M. R.; Teo, B. K.; Averill, B. A. *J. Am. Chem. Soc.* **1985**, *107*, 3583–3590.

(28) See, for example: Roe, A. L.; Schneider, D. J.; Mayer, R. J.; Pyrz, J. W.; Widom, J.; Que, L., Jr. *J. Am. Chem. Soc.* **1984**, *106*, 1676–1681.

(29) (a) Co, M. S.; Hodgson, K. O. In *Copper Proteins and Copper Enzymes*: Lontie, R. L. Ed.; CRC: Boca Raton, FL., 1984; Vol. 1, pp 93–113. (b) Cramer, S. P. *Adv. Inorg. Bioinorg. Mech.* **1983**, *2*, 259–316.

(30) (a) Shulman, R. G.; Yafet, Y.; Eisenberger, P.; Blumberg, W. E. *Proc. Natl. Acad. Sci. U.S.A.* **1976**, *73*, 1384–1388. (b) Hahn, J. E.; Scott, R. A.; Hodgson, K. O.; Doniach, S.; Desjardins, S. R.; Solomon, E. I. *Chem. Phys. Lett.* **1982**, *88*, 595–598.

Table I. Best-Fit Interatomic Distances and FABM Interatomic Distances and Coordination Numbers Obtained by Using Data Truncated at 1 and 11 $Å^{-1}$ and Fit over the Range 3–10 $Å^{-1}$ [d]

system	one-term fit		two-term fit		
	r (CN)[a]	χ^2	r_1 (CN)[a]	r_2 (CN)[a]	χ^2
$[Fe(HB(pz)_3)(O_2CCH_3)]_2O$	2.13	8.80	1.70	2.12	4.05
diffraction	2.10 (6.0)		1.78 (1.0)	2.12 (5.0)	
purple FePase	2.00	9.40	1.98	2.15	1.95
FABM[c]	1.97 (6.4)	24.35	1.98 (3.5)	2.13 (3.0)	6.80
pink FePase	2.09	5.16	2.01	2.17	1.75
FABM[c]	2.04 (6.9)	44.10	2.02 (2.2)	2.12 (3.8)	5.06

[a] r in Å; coordination number in parentheses. [b] The single-crystal diffraction data were obtained from ref 22a. [c] The coordination numbers were calculated via the FABM method, $N = B/S^*$, where S^* is the average characteristic amplitude reduction factor[26b,27c] obtained from $[Fe(HB(pz)_3)(O_2CCH_3)]_2O$. [d] The peak was isolated with a 1.0–2.4-Å window.

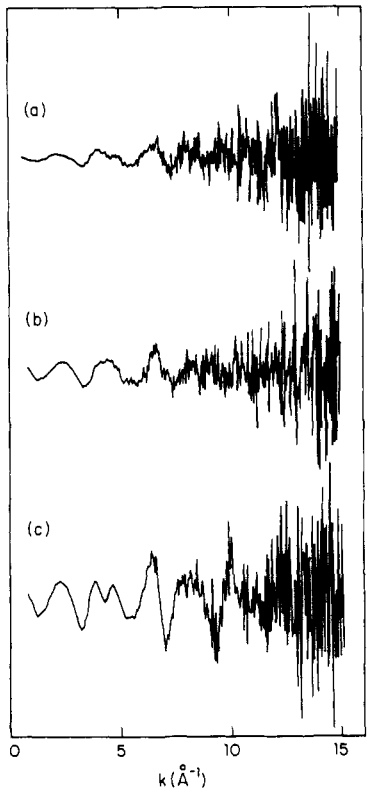

Figure 2. Background-removed K-edge EXAFS data: (a) pink FePase; (b) purple FePase; (c) $[Fe(HB(pz)_3)(O_2CCH_3)]_2O$ (V). The ordinate is an arbitrary scale.

in the last two systems. The intensity of this feature is thus very sensitive to the coordination geometry.[28] In Figure 1, compounds II and I (spectra c and d, respectively) are five-coordinate, and the intensities of the 1s → 3d transition are 6.3 and 9.0% respectively, of the main absorption edge. Compounds V and VI (Figure 1, spectra b and e, respectively) exhibit distorted octahedral geometry, and the intensities of the 1s → 3d peak are only 4.1 and 5.1%, respectively, of the main edge jump. These observations are in agreement with those of Co.[31] The 1s → 3d transition is visible for both the purple and pink forms of FePase (Figure 1), spectra f and a, respectively), and exhibits intensities of 4.3 and 4.2% of the main absorption edge, respectively. This suggests that the geometry around each of the iron atoms is pseudooctahedral (or possibly seven-coordinate[28]), with an inversion asymmetry. If the purple acid phosphatase contained one five-coordinate iron and one six-coordinate iron, the intensity of the 1s → 3d transition would be expected to be ~6–7% of the main absorption edge,[31] which is significantly larger than that observed. Note, however, that methemerythrin, which contains one 6-coordinate and one 5-coordinate iron atom,[32] exhibits a 1s → 3d transition that is only

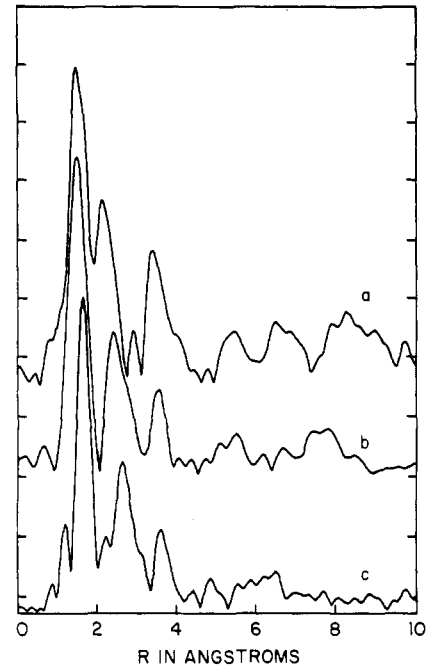

Figure 3. Fourier transforms of the K-edge EXAFS spectra: (a) pink FePase; (b) purple FePase; (c) $[Fe(HB(pz)_3)(O_2CCH_3)]_2O$ (V).

4–5% of the main absorption edge intensity.[33]

Extended X-ray Absorption Fine Structure. The measured EXAFS spectra and the results of the data analysis for the singly bridged μ-oxo model compounds I–IV were consistent with those reported by Co et al.,[34] and will not be discussed in detail. EXAFS data on the multiply bridged complex V have not been previously reported, and are compared to those of FePase below. In the FABM analysis[26b] of the protein data, complexes II and V were used as model compounds.

The background-removed EXAFS data for the purple and pink forms of FePase and for complex V are shown in Figure 2. For both forms of the enzyme, the EXAFS rapidly diminishes in intensity above $k \sim 11$ $Å^{-1}$. Consequently, the data were truncated at 1 and 12 $Å^{-1}$ and at 1 and 11 $Å^{-1}$ for the purple and pink forms of FePase, respectively, for analysis. Comparisons of the spectra of the purple and pink forms (e.g., Figures 2 and 3) utilize data truncated at 1 and 11 $Å^{-1}$ to permit direct comparison.

In Figure 3, the Fourier transforms of the EXAFS of the purple and pink forms of FePase are compared to that of complex V. Assignment of the peaks in the Fourier transform of V was straightforward, based on the published crystal structure.[22] The first peak, at $r' \sim 1.8$ Å, is due to O and N first-shell scatterers from the bridging oxo and acetate groups and the pyrazolates. After isolation via a Fourier filter ($r' = 1.0$–2.4 Å), the first shell could be fit with a single set of six O or N scatterers at 2.10 Å (FABM; best fit, 2.13 Å). The goodness of fit improved, however,

(31) Co, M. S. SSRL Report 84/02, 1983; pp 145–193.
(32) Stenkamp, R. E.; Sieker, L. C.; Jensen, L. H.; McCallum, J. D.; Sanders-Loehr, J. *Proc. Natl. Acad. Sci. U.S.A.* **1985**, *82*, 713–716.
(33) Sanders-Loehr, J. personal communication.
(34) Co, M. S.; Hendrickson, W. A.; Hodgson, K. O.; Doniach, S. *J. Am. Chem. Soc.* **1983**, *105*, 1144–1150.

Table II. Best-Fit Interatomic Distances and FABM Interatomic Distances and Coordination Numbers Obtained from the Fit to the Second Peak in the Fourier Transform[b]

system	r_{Fe-Fe} (CN)[a]	r_{Fe-X} (CN)[a,b]	χ^2
$[Fe(HB(pz)_3)(O_2CCH_3)]_2O$	3.09[c]		6.02
	3.14[d]	3.29[d,e]	0.460
	3.12[d]	2.94[d,f]	1.75
diffraction[g]	3.15 (1.0)	3.20 (6.0)	
purple FePase	3.00[c]		0.880
FABM[h]	3.01 (1.5)	3.03 (3.0)[e]	0.109
FABM[h]	3.00 (0.6)	3.06 (1.0)[f]	0.043

[a] r in Å; coordination number in parentheses. [b] X = C, P. [c] Single-term fit. [d] Two-term fit. [e] X = C. [f] X = P. [g] The single-crystal diffraction data were obtained from ref 22a. [h] The coordination numbers were calculated via the FABM method, $N = B/S^*$, where S^* is the average characteristic amplitude reduction factor[26b,27c] obtained from $[Fe(HB(pz)_3)(O_2CCH_3)]_2O$. [i] Data were truncated at 1 and 11 $Å^{-1}$ and fit over the range 3–10.5 $Å^{-1}$. The peak was isolated with a 2.0–3.2 Å window.

by 1 order of magnitude when a two-term fit with a short Fe–μ-oxo distance (1.78 Å, FABM; 1.70 Å, best fit) was included (Table I). Similarly, the second peak, at $r' \sim 2.7$ Å, was isolated by a Fourier filter ($r' = 2.0$–3.2 Å). It is due to a combination of Fe--Fe and Fe--C (second-shell) interactions (Table II). The Fe--Fe distance obtained in the two-term fit is 3.15 Å (FABM; best fit, 3.14 Å), in excellent agreement with the crystallographic value of 3.1457 (6) Å.[22b] Due to the Fe–O–Fe bridging angle of 123.6 (1)°, multiple-scattering effects are unimportant.[34,35] Use of a single Fe--Fe term gave a significantly shorter apparent Fe--Fe distance (3.09 Å). The final peak, at $r' \sim 3.6$ Å, is assigned to scattering from third-shell C atoms of the pyrazolate groups, by analogy with the focusing effect observed for imidazole complexes.[30a,36,37] After Fourier filtering ($r' = 3.1$–4.1 Å), fits using a single shell of carbon scatterers gave an Fe--C distance of 4.30 Å (FABM; best fit, 4.18 Å), in good agreement with that observed in other systems.[30a,36,37]

The Fourier transform of the EXAFS of the purple form of FePase (Figure 3) also consists of three major peaks, with the second exhibiting a definite shoulder whose resolution varied somewhat with the length of the data set and other experimental factors. The peaks are assigned as follows: Fe–O(N), first shell; Fe--Fe and Fe-P(C), second shell (see below); Fe--N(C) (imidazole), third shell.

After Fourier filtering ($r' = 1.0$–2.4 Å), the first peak (at $r' \sim 1.8$ Å) could fit by a single set of O(N) scatterers at 2.00 Å. A 5-fold improvement in goodness of fit resulted when two sets of O(N) scatterers were used (Table I). The coordination numbers obtained via the FABM method gave a set of three short and three longer Fe–O(N) distances, at 1.98 and 2.13 Å, respectively. In contrast to the results on hemerythrin[16] and on complex V, no evidence for a short Fe–μ-oxo distance of ~1.8 Å was observed. The probable presence of two Fe–O(tyrosine) bonds,[12–14] which are expected to exhibit bond lengths of 1.8–1.9 Å (on the basis of structurally characterized model complexes[38]), would cause significant overlap with the peak expected for a μ-oxo ligand and would result in a broader distribution of Fe–O(N) (first shell) distances in FePase than in the other systems. In addition, the available evidence[5,11a,14] suggests that both tyrosyl ligands are coordinated to the same iron atom, creating a significant asymmetry in the binuclear center of FePase compared to that of

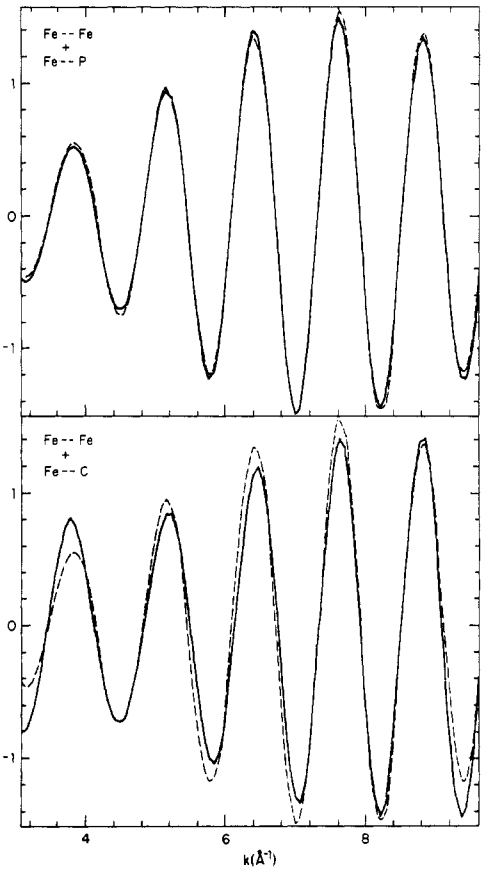

Figure 4. Best fits (solid lines) of the back-transformed second peak in the EXAFS of purple FePase, using Fe--Fe and Fe--P (top) and Fe--Fe and Fe--C (bottom) terms. Dashed lines represent experimental data.

hemerythrin or the model complexes. The observed Fe EXAFS is thus a superposition of the EXAFS of each of the Fe sites, which could well have slightly different ΔE_0's. Given these considerations, it is perhaps not surprising that direct evidence for a bridging oxo group was not obtained. It must, however, be emphasized that these results do *not* constitute evidence *against* the presence of a bridging oxo group. For example, in the EXAFS of II (which has a μ-oxo at 1.78 Å, two Fe–O at 1.93 Å, and two Fe–N at 2.14 Å[19]), the μ-oxo contribution could not be resolved either; instead, the best fit gave two distances ($r_1 = 1.90$ Å, $r_2 = 2.15$ Å).

After Fourier filtering ($r' = 2.0$–3.2 Å), the asymmetric second peak (at $r' \sim 2.4$ Å) in the Fourier transform of purple FePase was fit with both one term (Fe--Fe) and two terms (Fe--Fe, Fe--C or Fe--Fe, Fe--P); the results are given in Table II. The Fe--Fe distance observed in both fits is remarkably short (3.00 Å). This implies a rather small Fe–O–Fe angle (ca. 115°), if a bridging oxo is indeed present, and is most consistent with a multiply bridged structure such as that of V[22] (Fe--Fe, 3.1457 (6) Å; Fe–O–Fe, 123.611 (1)°) and $[Fe_2(tacn)_2(O_2CCH_3)_2O]$[39] (Fe--Fe, 3.064 (5) Å; Fe–O–Fe, 118.3 (5)°) (tacn = 1,4,7-triazacyclononane). Such a small Fe–O–Fe angle would explain the lack of significant enhancement of the Fe--Fe peak in the EXAFS.[34,35] A short Fe--Fe distance is also consistent with the strong antiferromagnetic coupling observed.[9]

Inclusion of a second term of low Z scatterers (e.g., C) resulted in a substantial improvement in the fit to the data. Similar improvement has been noted in the analysis of hemerythrin EXAFS data.[33] Because of the presence of firmly bound phosphate in purple FePase,[15c] however, a two-term fit with an Fe--P rather than Fe--C term was also examined, and gave a significantly better fit (Figure 4, Table II). Although Fe--C (second shell) interactions are almost certainly present (in addition to the Fe--P interaction), no attempt was made to utilize a three-term (Fe--Fe,

(35) Teo, B. K. *J. Am. Chem. Soc.* **1981**, *103*, 3990–4001.
(36) Bunker, G.; Stern, E. A.; Blankenship, R. E.; Parson, W. W. *Biophys. J.* **1982**, *37*, 539–551.
(37) (a) Co, M. S.; Hodgson, K. O.; Eccles, T. K.; Lontie, R. *J. Am. Chem. Soc.* **1981**, *103*, 984–986. (b) Co, M. S.; Scott, R. A.; Hodgson, K. O. *J. Am. Chem. Soc.* **1981**, *103*, 986–988.
(38) (a) White, L. S.; Nilsson, P. V.; Pignolet, L. H.; Que, L., Jr. *J. Am. Chem. Soc.* **1984**, *106*, 8312–8313. (b) Heistand, R. H., II; Roe, A. L.; Que, L., Jr. *Inorg. Chem.* **1982**, *21*, 676–681. (c) Lauffer, R. B.; Heistand, R. H., II; Que, L. Jr. *Inorg. Chem.* **1983**, *22*, 50–55. (d) Cleland, W. E.; Holtman, D. A.; Sabat, M.; Ibers, J. A.; DeFotis, G. C.; Averill, B. A. *J. Am. Chem. Soc.* **1983**, *105*, 6021–6031.
(39) Wieghardt, K.; Pohl, K.; Gebert, W. *Angew. Chem., Int. Ed. Engl.* **1983**, *22*, 727.

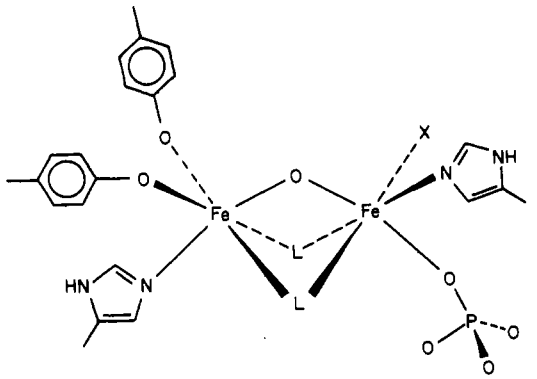

Figure 5. Proposed model for the binuclear iron site of purple acid phosphatases, based on EXAFS (this work), NMR,[14] resonance Raman,[12,13] and magnetic susceptibility[9,10c] results. L indicates possible bridging groups in addition to a μ-oxo. X indicates an unidentified ligand.

Fe--P, Fe--C) fit. Similar two-term fits were examined for complexes I–V, and in all cases the fit with an Fe--C term was significantly better than with Fe--P, as expected. These results suggest the presence of an Fe--P interaction at ~3.06 Å in the purple form of FePase and are consistent with the presence of a phosphate bound to iron with an Fe–O–P angle of ca. 125°. The observed Fe--P distance is significantly shorter than that in a bis(phosphodiester)-bridged binuclear Fe(III) complex (~3.21 Å[40]) and that inferred by EXAFS in a polynuclear Fe(III)–ATP complex (3.27 Å[41]). For comparison, the bidentate phosphate ligand in $[(en)_2CoPO_4]$ exhibits a Co--P distance of 2.544 Å and a Co–O–P angle of 92.7,[42] while monodentate phosphate residues in a series of cobalt(III)–ammine–phosphate complexes exhibit Co–P distances of 3.09–3.22 Å and Co–O–P angles of 126–139°.[43] These results suggest that the phosphate in purple FePase is ligated to a single Fe atom in a monodentate fashion.

The final peak (at $r' \sim 3.6$ Å) in the Fourier transform of purple FePase was isolated by a Fourier filter ($r' = 3.1$–4.1 Å). The amplitude of this peak appears to be enhanced. It was fit with a single term, giving an Fe--C(N) distance of 4.3 Å. The focusing effect in metal–imidazole derivatives is well-documented,[36,37,44] and these results provide convincing evidence confirming the presence of histidine imidazole ligands to iron, as suggested by ^{1}H NMR studies.[14]

The Fourier transform of the EXAFS of the pink form of FePase (Figure 3) is similar to that of the purple form, except for the second peak, which is clearly resolved into an intense peak at $r' = 2.4$ Å and a weak peak at 2.9 Å. The first peak was isolated with a Fourier filter (1.0–2.4 Å) and fit with both one term and two terms (Table I). The two-term fit gave a χ^2 value approximately 10 times better than that with a single term (FABM results). Upon reduction of FePase from purple to pink, the overall coordination number of the iron sites remains unchanged, but the average Fe–O(N) distance increases by ca. 0.06 Å. This is expected on the basis of trends in ionic radii.[45] More important, however, is the change in the distribution of bond lengths within the first coordination sphere. The purple form has three to four O (N) atoms at short distances (≤2 Å), while this number decreases to only two in the pink form. These results are consistent with either loss of or protonation of a short Fe–μ-oxo group.[32,46]

The second and third peaks in the Fourier transform of pink FePase, at ~2.2 and 2.9 Å, were Fourier-filtered as a unit ($r' = 1.9$–3.1 Å). The large peak at $r' = 2.2$ Å dominates this portion of the EXAFS and could be adequately fit as two sets of Fe--C neighbors, at 2.59 and 2.94 Å. The small peak at $r' = 2.9$ Å is tentatively assigned to the Fe--Fe interaction. Since it makes only a minor contribution to the EXAFS, its inclusion in fits was not particularly useful. The absence of a significant Fe--Fe peak is similar to the behavior of deoxyhemerythrin,[16b] where only a very small peak is observed for the Fe--Fe interaction at high temperatures. This type of behavior has been attributed to an increase in Debye–Waller factors due to uncorrelated vibrations of the two Fe atoms.[16b] Loss of or protonation of a bridging group is expected to result in a less tightly coupled pair of iron atoms and is a reasonable explanation for the behavior observed in the pink FePase as well. The final peak in the Fourier transform of pink FePase (at $r' \sim 3.8$ Å) is very similar to that observed for the purple form and is also assigned to enhanced scattering by imidazole C(N)'s at ~4.3 Å.

Conclusions

The near-edge absorption data suggest that both iron atoms in oxidized (purple) and reduced (pink) bovine spleen purple acid phosphatase are in six-coordinate sites of relatively low symmetry. Reduction of the enzyme results in a shift of the absorption edge to lower energy by 2.0 eV. The EXAFS does not provide evidence for a short (~1.8 Å) Fe–μ-oxo bond, probably due to interference by short Fe–O(tyrosine) bonds at 1.8–1.9 Å. The average first-shell distances obtained for the purple form of the enzyme are short compared to those observed for hemerythrin or multiply bridged model complexes, consistent with the presence of several scatterers at relatively short distances in the former. The observed Fe--Fe distance of 3.00 Å for the purple form of the enzyme implies an angle of ca. 115° at the bridging oxo (if present). This is not an unreasonable value and would account for the lack of enhancement of the amplitude of the Fe--Fe peak. The EXAFS of the purple form also provides direct evidence for the presence of a phosphate coordinated to one of the iron atoms, which is absent in the pink form. Available data from all spectroscopic techniques utilized to date are consistent with the structural model shown in Figure 5; the bridging ligands L may be carboxylates, by analogy to hemerythrin. Studies are in progress on the molybdate-inhibited enzyme, which should allow us to unequivocally assign the phosphate peak, and on metal-substituted enzymes (e.g., the FeZn enzyme[9]), which will allow us to determine which metal site interacts with inhibitors and, presumably, substrate.

Acknowledgments. This research was supported by grants from the National Institutes of Health (GM 28636 and GM 32117) to B.A.A. We thank M. R. Antonio, P. Lindahl, A. Nagahisa, C. Hulse, and O. Fussâ, who at various times helped with data collection. We thank the CHESS staff for their assistance and J. Sanders-Loehr for helpful discussions.

Registry No. I, 51331-59-0; II, 36379-64-3; IV, 47821-83-0; V, 86177-70-0; FePase, 9001-77-8; Fe, 7439-89-6; PO_4, 14265-44-2.

Supplementary Material Available: Plots of X-ray absorption data for the purple and pink forms of FePase and plots of Fe–O(N) single-term and two-term fits (6 pages). Ordering information is given on any current masthead page.

(40) Armstrong, W. H.; Lippard, S. J. *J. Am. Chem. Soc.* **1985**, *107*, 3730–3731.
(41) Mansour, A. N.; Thompson, C.; Theil, E. C.; Chasteen, N. D.; Sayers, D. E. *J. Biol. Chem.* **1985**, *260*, 7975–7979.
(42) Anderson, B.; Milburn, R. M.; Harrowfield, J. MacB.; Robertson, G. B.; Sargeson, A. M. *J. Am. Chem. Soc.* **1977**, *99*, 2652–2661.
(43) Merrit, E. A.; Sundaralingam, M. *Acta Crystallogr., Sect. B: Struct. Crystallogr. Cryst. Chem.* **1980**, *B36*, 2576–2584.
(44) Felton, R. H.; Barrow, W. L.; May, S. W.; Sowell, A. L.; Geol, S.; Bunker, G.; Stern, E. A. *J. Am. Chem. Soc.* **1982**, *104*, 6132–6134.
(45) (a) Shannon, R. D.; Prewitt, C. T. *Acta Crystallogr., Sect. B: Struct. Crystallogr. Cryst. Chem.* **1969**, *B25*, 925–946. (b) Shannon, R. D. *Acta Crystallogr., Sect. A: Cryst. Phys., Diffr., Theor. Gen. Crystallogr.* **1976**, *A32*, 751–767.
(46) Armstrong, W. H.; Lippard, S. J. *J. Am. Chem. Soc.* **1984**, *106*, 4632–4633.